Bounding Network-Induced Delays of Wireless PRP Infrastructure for Industrial Control Systems

Huan Yang* and Liang Cheng†
Department of Computer Science and Engineering, Lehigh University, Bethlehem, Pennsylvania 18015
Email: huy213@lehigh.edu*, cheng@cse.lehigh.edu†

***Abstract*—Recently, wireless communication technologies, such as Wireless Local Area Networks (WLANs), have gained increasing popularity in industrial control systems (ICSs) due to their low cost and ease of deployment, but communication delays associated with these technologies make it unsuitable for critical real-time and safety applications. To address concerns on network-induced delays of wireless communication technologies and bring their advantages into modern ICSs, wireless network infrastructure based on the Parallel Redundancy Protocol (PRP) has been proposed. Although application-specific simulations and measurements have been conducted to show that wireless network infrastructure based on PRP can be a viable solution for critical applications with stringent delay performance constraints, little has been done to devise an analytical framework facilitating the adoption of wireless PRP infrastructure in miscellaneous ICSs. Leveraging the deterministic network calculus (DNC) theory, we propose to analytically derive worst-case bounds on network-induced delays for critical ICS applications. We show that the problem of worst-case delay bounding for a wireless PRP network can be solved by performing network-calculus-based analysis on its non-feedforward traffic pattern. Closed-form expressions of worst-case delays are derived, which has not been found previously and allows ICS architects/designers to compute worst-case delay bounds for ICS tasks in their respective application domains of interest. Our analytical results not only provide insights into the impacts of network-induced delays on latency-critical tasks but also allow ICS architects/operators to assess whether proper wireless RPR network infrastructure can be adopted into their systems.**

***Index Terms*—Wireless PRP network infrastructure, deterministic network calculus, non-feedforward networks, worst-case delay analysis, network-induced delays, Parallel Redundancy Protocol, industrial control systems.**

I. Introduction

Due to their low cost and ease of deployment as well as maintenance, wireless communication technologies, such as Wireless Local Area Networks (WLANs), have become an attractive communication solution for industrial control systems (ICSs) [1], [2]. However, many wireless communication protocols are not initially proposed for ICSs requiring reliable and low-latency communication. For instance, the IEEE 802.11 family of WLANs are primarily designed to offer high throughput and continuous connectivity. Reliability and latency issues caused by radio interference have become a major deterrent to the application of WLANs in ICSs with latency-critical tasks [3]. To address these concerns, the Parallel Redundancy Protocol (PRP) [4] is leveraged to construct dependable wireless network infrastructure for real-time and safety ICS applications. As an example, parallel

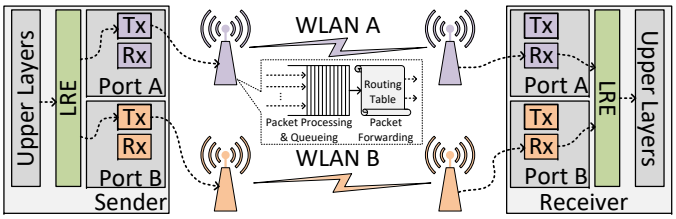

Fig. 1. A simplified view of a parallel redundant WLAN [5], [6]. The link redundancy entity (LRE) layer replicates the frame sent by the sender and discards the duplicate frame at the receiver.

redundant WLANs [5], [6] are proposed to compensate the effects of stochastic channel fading by parallel operation of diverse wireless channels, resulting in a fault-tolerant wireless network infrastructure for ICSs with latency-critical and safety applications. Fig. 1 presents a simplified view of a parallel redundant WLAN with unidirectional network traffic from a sender to a receiver. When the sender generates a data frame, its link redundancy entity (LRE) layer duplicates the frame and forwards it via both WLANs A and B. At the receiver side, the LRE layer removes the duplicate that arrives late, forwarding only a single copy to the upper layers. Using PRP as splitter and selection combiner, parallel redundant WLANs offer an improved wireless communication infrastructure with high stochastic reliability. Although wireless PRP networks such as parallel redundant WLANs provide a viable and reliable wireless communication solution for networked control systems (NCSs), application-specific delay performance evaluation is still required (e.g., [7], [8]) because different ICS tasks and applications have diverse delay performance requirements (e.g., constraints on worst-case network-induced delays for various power substation automation tasks are specified in [9]).

Application-specific delay performance of wireless PRP infrastructure is heretofore studied through discrete-event simulations (e.g., [8], [10]) and/or measurements (e.g., [7], [11]). These approaches enable ICS architects to evaluate the feasibility and usability of wireless PRP infrastructure for specific ICSs of interest during the planning phase of ICS design, but new simulation/experiment must be conducted when important modifications to the ICS design (e.g., changing the sampling frequencies of sensors) are introduced or the same set of equipment are employed in new ICS designs. To reuse measurement and simulation results and reduce the cost of delay performance evaluation, it is of vital importance to develop a theoretical framework that allows ICS architects to

quickly assess whether certain latency-critical applications can be run on wireless PRP networks.

In this paper, we propose a network-calculus-based framework to analyze worst-case network-induced delays of wireless network infrastructure based on PRP, facilitating its adoption in miscellaneous ICSs with diverse delay performance requirements. Contributions of this work are as follows:

- *Modeling Wireless PRP Networks with Network Calculus.* Leveraging the deterministic network calculus (DNC) theory, we model wireless PRP networks to capture the impacts of various components of network-induced delays, including processing delays, transmission delays, and queueing delays. The proposed models enable ICS architects/designers to reuse application-specific delay measurements or simulation results and estimate worst-case delay performance of wireless PRP networks in new ICS designs.
- *Delay Bounding on Non-Feedforward Networks.* Practical wireless PRP networks support bidirectional communication between senders and receivers (see Sec. III-E), which results in non-feedforward traffic patterns that cannot be handled by state-of-the-art delay bounding techniques designed for feedforward traffic pattern (i.e., all traffic flows on a network can be represented by increasing sequences after unique integer identifiers are assigned to all network nodes [12]). In this work, we address this challenge by introducing stopped sequences into our worst-case delay analysis framework and make our proposed approach applicable to realistic application scenarios of wireless PRP networks.
- *Derivation of Closed-Form Worst-Case Delay Expressions.* We demonstrate that our proposed approach is able to derive closed-form expressions of worst-case network-induced delays under general, non-feedforward network traffic patterns. The closed-form expressions can be re-used in different phases of ICS design as long as the given network traffic pattern remains the same. The proposed framework is thus a valuable tool for ICS architects aiming to design wireless PRP network infrastructure for latency-critical ICSs.

II. Related Work

A. Wireless PRP Network Infrastructure

Proposed and evaluated in [5], [6], parallel redundant WLANs have been shown to offer satisfactory reliability for real-time and safety applications in industrial control systems. In [11], [13], seamless redundancy principles of PRP are directly applied to WLAN links and additional improvements such as duplication avoidance mechanisms are designed in the proposed Wi-Red protocol. To ensure that communication delays induced by parallel redundant WLANs can be tolerated by critical ICS tasks, discrete-event simulations and measurement-based experiments have been conducted for various industrial control applications, such as power system state estimation using phasor measurement data [7] and wireless networked control systems for industrial workcell [8]. However, network-induced delays obtained through simulation or measurement are typically not the worst-case results because the testing scenarios are constructed based on representative communication workloads but do not exhaustively cover boundary cases that can lead to significant increase in network-induced delays. Furthermore, when modifications to an ICS design result in traffic pattern changes or a new ICS is to be designed, previously obtained results cannot be re-used and new experiments/simulations must be conducted. This problem can be resolved by the development of a theoretical framework for worst-case delay analysis of wireless PRP networks, which is the major contribution of this work.

In addition to WLANs, PRP has also been combined with other wireless communication technologies. Leveraging 4G Long Term Evolution (LTE) cellular protocol, a wireless seamless redundant communication infrastructure is proposed for railway communication systems in [14]. To facilitate flexible factory automation and control, seamless redundancy principles of PRP are applied to IEEE 802.15.4 wireless networks in [15]. Though the combination of wireless communication technologies and PRP leads to flexible and reliable wireless communication infrastructure for ICSs, these solutions need to be carefully evaluated for different latency-critical tasks before adoption/deployment. The worst-case delay analysis framework proposed in this paper can be applied to different wireless PRP networks, ranging from wireless redundant WLANs to those based on 4G LTE or IEEE 802.15.4, reducing the cost of delay performance evaluation for ICS design.

B. Worst-Case Delay Performance Analysis Using Network Calculus

In contrast to queueing theory, network calculus [16]–[18] studies worst-case performance of queueing networks. To apply network-calculus theorems and derive delay bounds for networks with different topologies, many algorithms have been proposed and implemented. In [19], three different algorithmic approaches to applying network-calculus theorems, namely total-flow analysis (TFA), separated-flow analysis (SFA), and pay-multiplexing-only-once (PMOO) analysis, are developed for wireless sensor networks (WSNs). It has later been shown in [20] that these algorithms may not always generate tight delay bounds. To derive tighter delay bounds by combining the TFA, SFA, and PMOO approaches, a new delay bounding method [21] has been proposed. However, computational cost of this approach is prohibitively expensive. Alternatively, the problem of worst-case delay analysis can be formulated as optimization problems under network-calculus constraints [12], [20]. However, the computational costs of the optimization-based approaches may be prohibitively high [12] if exact (i.e., tight) delay bounds are desired.

Existing algorithms of network-calculus-based worst-case delay analysis focus on tightening the delay bounds for feedforward networks. A network is said to be feedforward if all its traffic flows can be represented by increasing sequences after unique integer identifiers are assigned to all the network

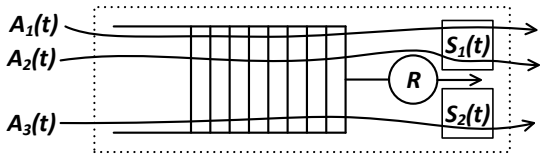

Fig. 2. Network-calculus model of a single wireless access point on a wireless PRP network.

nodes. If no feasible assignment scheme can be found (i.e., at least one of the traffic flows cannot be represented by an increasing sequence under any assignment scheme), the network is regarded as non-feedforward. Traffic patterns resulted from bidirectional communication on wireless PRP networks are non-feedforward, making existing algorithms inapplicable. In this paper, we propose to apply network calculus theorems to non-feedforward traffic patterns, making it possible to derive delay bounds for practical wireless PRP networks.

III. Modeling Wireless PRP Networks with Network Calculus

The key to applying network calculus to wireless PRP networks is to properly model all the traffic forwarding devices (e.g., wireless access points, 4G LTE base stations, or IEEE 802.15.4 sensor nodes). Throughout the remainder of this paper, we present our proposed framework using wireless redundant WLANs as an example. We note that the same modeling approach can be applied to other wireless PRP network infrastructure (see Sec. II-A) as well.

A wireless access point (AP) in parallel redundant WLANs (e.g., see Fig. 1) can be modeled by a constant-capacity work-conserving link with ideal routers attached to its output end. At each wireless access point, a packet must go through certain processing tasks (e.g., validating its CRC bytes). If the communication channel is temporarily not available for transmission, the packet needs to be queued. When the communication channel becomes available, the packet is forwarded to the destination according to one of the routing table entries. In our proposed framework, packet processing and queueing at an access point is modeled by a work-conserving link, whereas the routing table entry designating the forwarding of packets in a traffic flow toward a certain destination node is modeled by an ideal router. Since a traffic flow originating from a source node may be forwarded to multiple destinations, multiple ideal routers are attached to the work-conserving link to represent all relevant routing table entries.

As an example, let us consider the AP model in Fig. 2. The work-conserving link has capacity R and receives three individual input flows $A_1(t)$, $A_2(t)$, and $A_3(t)$. The control functions of the two ideal routers are $S_1(t)$ and $S_2(t)$, respectively. Each control function can be thought as a routing table entry, which specifies whether a packet can pass through the router or not. The ensuing subsections introduce the important theorems and concepts from network calculus that are used in our proposed analytical framework. Formal proofs of the theorems can be found in classic textbooks on network calculus, such as [17], [18].

A. Definitions

In network calculus, arrival and departure processes (i.e., traffic flows) are modeled by non-negative cumulative functions. A cumulative function $A(t)$ is a non-negative and non-decreasing function defined for $t \geq 0$ with $A(0) = 0$. If an arrival process is modeled by $A(t)$, then $A(t_1)$ represents the cumulative traffic volume seen from this process starting from $t=0$ up until $t=t_1$.

In addition, arrival curves are used in network calculus to characterize traffic flows. For a traffic flow modeled by cumulative function $A(t)$, a function $\alpha(t)$ is the arrival curve for $A(t)$ if and only if

$$A(t) - A(s) \leq \alpha(t-s), \text{ for } \forall t \geq s \geq 0.$$

A widely-used type of arrival curves is the leaky-bucket arrival curve, which is of the form $\alpha(t)=\rho t+\sigma$. If a traffic flow $A(t)$ has an arrival curve $\alpha(t)=\rho t+\sigma$, then it is said to be (σ, ρ)-upper constrained, which is denoted by $A\sim(\sigma, \rho)$. Parameter ρ represents the long-term average rate of $A(t)$, whereas σ represents the (maximum) instantaneous burstiness of $A(t)$.

In network calculus, networking devices such as wireless access points are modeled by network elements offering certain service curves. Suppose that a network element has a single arrival process $A(t)$ and a single departure process $D(t)$. The network element is said to offer a service curve $\beta(t)$ if and only if

$$D(t) \geq \inf_{0 \leq s \leq t} \{A(s) + \beta(t-s)\} = (A \otimes \beta)(t), \text{ for } \forall t \geq 0.$$

The operator $\otimes$ denotes the min-plus convolution operation. If a work-conserving link has constant capacity R, then we say that its service curve is $\beta(t)=R \cdot t$.

An input flow may be routed (i.e., demultiplexed) to multiple output paths. An ideal router is a network element with traffic input $A(t)$, output $D(t)$, and control input $F(t)$. The input-output relationship between the input flow to an ideal router and its output flow governed by $F(t)$ is expressed as $D(t)=F[A(t)]$. Note that an input flow can pass through multiple ideal routers when its packets have different destinations.

B. Modeling Traffic Forwarding Devices

To facilitate back-of-the-envelop calculation, we model a wireless access point in parallel redundant WLANs using a constant-capacity work-conserving link with ideal routers attached to its output end. This subsection introduces two key operations used in the construction of the model illustrated in Fig. 2 for a wireless access point.

1) Traffic Aggregation: Suppose that multiple input flows are fed into a single wireless access point (e.g., multiple senders running different control tasks instead of single sender shown in Fig. 1 can be connected to the same wireless access point). If $A_1\sim(\sigma_1, \rho_1)$ and $A_2\sim(\sigma_2, \rho_2)$, then the aggregation of $A_1(t)$ and $A_2(t)$, namely $A_1(t) + A_2(t)$, is said to be $(\sigma_1+\sigma_2, \rho_1+\rho_2)$-upper constrained. In general, we have the following lemma for traffic aggregation (also known as traffic flow multiplexing).

Lemma 1: Suppose that a network element has n input flows $A_i(t), i=1,2,\ldots,n$. If each individual flow A_i is (σ_i,ρ_i)-upper constrained, then the aggregation of the n input flows is represented by $A(t)=\Sigma_{i=1}^{n}A_i(t)$ and is $(\Sigma_{i=1}^{n}\sigma_i,\Sigma_{i=1}^{n}\rho_i)$-upper constrained.

When two traffic flows merge, their data bits will be serialized according to a certain multiplexing policy. Note that this serialization effect is not modeled by Lemma 1. Combining traffic flows sharing the same ideal router or destined for the same next-hop wireless access point using this lemma simplifies the derivation of worst-case delay bounds for non-feedforward networks and makes back-of-the-envelop calculation possible.

2) Left-Over Service Curve: The notion of left-over service curve has been extensively used in delay-bounding algorithms for feedforward networks such as those proposed in [19]–[21]. In our analytical framework, we also leverage the following theorem for left-over service curve.

Theorem 2: Suppose that a work-conserving link has constant capacity R and two inputs $A_1(t)$ and $A_2(t)$. If $A_1\sim(\sigma_1,\rho_1)$, then the service curve offered by this work-conserving link to $A_2(t)$ can be denoted by $\beta_2(t)$, where $\beta_2(t)=(Rt-\rho_1 t-\sigma_1)^+$, and $(\cdot)^+$ is defined as $\max\{\cdot,0\}$.

As illustrated in Fig. 2, packet-processing elements of a wireless access point are modeled using a single work-conserving link with constant capacity R and infinite buffers (so that no packets are dropped due to buffer overflow). We note that this single-link model is conservative because parallelisms inside the wireless access point are ignored. Instead, we assume that the wireless access point processes packets one by one when multiple packets arrive simultaneously or when its buffer is not empty. Theorem 2 allows us to find out the service curve solely used by an individual flow (though this flow itself may be an aggregation of multiple flows). The service curve obtained from this theorem is known as left-over service curve [20].

C. Output Burstiness and Worst-Case Delay

Theorem 3: Suppose that a network element offers service curve $\beta(t)$ for input flow $A(t)$. The output flow corresponding to $A(t)$ is denoted as $D(t)$. If $A(t)$ has an arrival curve $\alpha(t)$, then $D(t)$ has an arrival curve $\alpha'(t)$, where

$$\alpha'(t)=\sup_{t,s\geq 0}\{\alpha^*(t+s)-\beta(s)\}=(\alpha^*\oslash\beta)(t).$$

Note that $\alpha^*(t)$ is the sub-additive closure of $\alpha(t)$ and the $\oslash$ operator denotes the deconvolution operation. Definition of sub-additive closure can be found in [17], [18]. For a leaky-bucket arrival curve $\alpha(t)=\rho t+\sigma$, we have $\alpha^*(t)=\alpha(t)$.

In addition, we have the following theorem for worst-case delay experienced by a single flow passing through a networking element that offers service curve $\beta(t)$.

Theorem 4: Suppose that a network element offers service curve $\beta(t)$ to its input flow $A(t)$, which has an arrival curve $\alpha(t)$. Let $d(t)$ denote that maximum delay experienced by flow $A(t)$ up to time t, the worst-case delay bound can be found as follows

$$\forall t\geq 0:\ d(t)\leq\inf\{t\geq 0:\ (\alpha^*\oslash\beta)(-t)\leq 0\}.$$

D. Ideal Routing

The behavior that a wireless access point routes packets from its input flow to different destinations can be modeled using ideal routers. To model bidirectional communications on parallel redundant WLANs, we need to consider multiple traffic flows passing through a wireless access point and arriving at different destinations. As shown in Fig. 2, we attach two ideal routers to the output end of the work-conserving link. Each router routes part of the flow passing through it toward a wireless access point. The following lemma can be applied when ideal routers are introduced.

Lemma 5: Suppose that an ideal router has a single input $A(t)$, which is (σ,ρ)-upper constrained. If the routing control function $F(t)$ is (δ,γ)-upper constrained, then its output flow $D(t)$ is $(\gamma\sigma+\delta,\gamma\rho)$-upper constrained.

We only show the ideal routers relaying packets towards other wireless access points in Fig. 2 because our flows of interest are the aggregated flows passing through two wireless access points to travel from a sender to a receiver (see Fig. 1).

E. Non-Feedforward Traffic Patterns and Stopped Sequences

In practical applications of wireless PRP networks, bidirectional communications between a sender and a receiver typically result in a non-feedforward traffic pattern. For any given network, we can assign unique integer identifiers to all its network nodes and represent all the traffic flows as integer sequences. If no feasible assignment scheme can be found such that all the flows can be represented as monotonically increasing sequences, the network has a non-feedforward traffic pattern.

1) Modeling a Single Wireless Path of Wireless PRP Networks: Fig. 3 illustrates the model for a wireless path of a parallel redundant WLAN with a non-feedforward traffic pattern. In particular, $C_1(t)$ and $D_1(t)$ models the aggregated traffic flows passing through individual wireless access points (APs) and getting forwarded toward destinations other than the two APs connecting the sender and the receiver (e.g., the sender may send data frames to APs other than the ones connecting the sender and the receiver, and so does the receiver). On the path of $A_1(t)$, two ideal routers are inserted so that $A_5(t)$ represents aggregated traffic flow consumed by the receiver connected to wireless AP2. Similarly, two ideal routers are inserted so that $B_5(t)$ models the traffic flow consumed by the receiver connected to the wireless AP1 (since we consider practical scenarios with bidirectional communications). Note that the sender connected to AP1 is one of the sources contributing to the aggregated input flow $A_1(t)$. Similarly, the sender connected to AP2 is among the sources that generate $B_1(t)$. Evidently, the non-feedforward traffic pattern is caused by the bidirectional communications between the sender and the receiver: To determine the left-over service curve offered by AP1 for A_1, we have to determine the arrival curve for $B_3(t)$, which in turn requires the determination of the left-over service curve offered by AP2 for $B_1(t)$. However, to determine this left-over service curve for $B_1(t)$, we need to obtain the arrival curve of $A_3(t)$, which in turn requires the

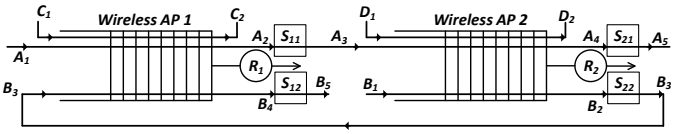

Fig. 3. Modeling of a wireless path of a wireless PRP network with a non-feedforward traffic pattern imposed by bidirectional communications between sender and receiver attached to different wireless access points (APs).

determination of the left-over service curve offered by AP1 for $A_1(t)$. Such intricacies will not be encountered if the traffic pattern is feedforward (i.e., all traffic flows on the network can be represented by a set of increasing sequences by properly assigning integer identifiers to all the networking nodes [12]), but it is necessary to derive worst-case delay bounds on non-feedforward networks because practical parallel redundant WLANs are generally non-feedforward.

2) Stopped Sequences: To analyze such a non-feedforward traffic pattern, we use the technique of introducing stopped sequences. For a cumulative function $A(t)$, cumulative function $A^\tau(t)$ is the stopped sequence of $A(t)$ at time $\tau \geq 0$ and is defined as

$$A^\tau(t) = \begin{cases} A(t), & \text{if } t \leq \tau, \\ A(\tau), & \text{otherwise.} \end{cases}$$

The following two lemmas enable us to analyze non-feedforward traffic patterns and find out whether worst-case end-to-end delay bounds exist.

Lemma 6: For every chosen ρ, a stopped sequence $A^\tau(t)$ is $(\sigma(\tau), \rho)$-upper constrained, where

$$\sigma(t) = \sup_{0 \leq t \leq \tau} \sup_{0 \leq s \leq t} \{A(t) - A(s) - \rho(t-s)\}.$$

Lemma 7: If the stopped sequence $A^\tau(t)$ in Lemma 6 is also found to be (σ, ρ)-upper constrained, then we have $\sigma(\tau) \leq \sigma$.

IV. Worst-Case Delay Analysis for Wireless PRP Network Infrastructure

With the concepts, theorems, and lemmas introduced in Section III, we now fully parameterize the model depicted in Fig. 3 and show the existence of upper bounds on the end-to-end delays induced by this wireless path. In particular, we derive the worst-case delay experienced by packets that are sent to the receiver connected to AP2 by the sender connected to AP1. Leveraging symmetry of the non-feedforward traffic pattern, worst-case delays experienced by packets sent by the sender at AP2 to the receiver at AP1 can be derived similarly. Note that for a practical parallel redundant WLAN, two wireless paths need to be modeled and analyzed. The parameters for the models will have different values, which can be obtained from prior measurements or simulations.

Suppose that all input flows have leaky-bucket arrival curves. Without loss of generality, suppose that we have $A_1 \sim (\sigma_{A1}, \rho_{A1})$, $B_1 \sim (\sigma_{B1}, \rho_{B1})$, $C_1 \sim (\sigma_{C1}, \rho_{C1})$, and $D_1 \sim (\sigma_{D1}, \rho_{D1})$ for the input flows. We also assume that both APs have sufficient processing capacity, i.e., $R_1 > \rho_{A1} + \rho_{B1} + \rho_{C1}$ and $R_2 > \rho_{A1} + \rho_{B1} + \rho_{D1}$. To model bidirectional communications, the output end of each work-conserving link is attached with two ideal routers. S_{11}, S_{12}, S_{21}, and S_{22} are the control functions of the ideal routers, respectively. Suppose that we have $S_{11} \sim (\delta_{11}, \gamma_{11})$, $S_{12} \sim (\delta_{12}, \gamma_{12})$, $S_{21} \sim (\delta_{21}, \gamma_{21})$, and $S_{22} \sim (\delta_{22}, \gamma_{22})$. We note that values of the parameters introduced here can be obtained either from prior knowledge of traffic profiles of different ICS applications or from measurements and simulations.

Since this traffic pattern is non-feedforward, we introduce stopped sequences for all the traffic flows. For instance, A_2^τ and B_2^τ are the stopped sequences for flows A_2 and B_2, respectively. Applying Lemma 6, we can have $A_2^\tau \sim (\sigma_{A2}(\tau), \rho_{A1})$ and $B_2^\tau \sim (\sigma_{B2}(\tau), \rho_{B1})$. Applying Lemma 5 at ideal routers S_{11} and S_{22}, we have $A_3^\tau \sim (\gamma_{11}\sigma_{A2}(\tau) + \delta_{11}, \gamma_{11}\rho_{A1})$ and $B_3^\tau \sim (\gamma_{22}\sigma_{B2}(\tau) + \delta_{22}, \gamma_{22}\rho_{B1})$. At AP1, we apply Theorem 2 and Lemma 1 to obtain the left-over service curve for A_1, which is denoted by $\beta_{A1}^\tau(t)$ and

$$\beta_{A1}^\tau(t) = (R_1 t - (\rho_{C1} t + \sigma_{C1} + \gamma_{22}\sigma_{B2}(\tau) + \delta_{22} + \gamma_{22}\rho_{B1} t))^+.$$

Similarly, we also have

$$\beta_{B1}^\tau(t) = (R_2 t - (\rho_{D1} t + \sigma_{D1} + \gamma_{11}\sigma_{A2}(\tau) + \delta_{11} + \gamma_{11}\rho_{A1} t))^+.$$

Then, by applying Theorem 3 on A_1 and $\beta_{A1}^\tau(t)$, we have $A_2^\tau \sim (\sigma'_{A2}(\tau), \rho_{A1})$, where

$$\sigma'_{A2}(\tau) = \sigma_{A1} + \rho_{A1} \cdot \frac{\sigma_{C1} + \gamma_{22}\sigma_{B2}(\tau) + \delta_{22}}{R_1 - \rho_{C1} - \gamma_{22}\rho_{B1}}.$$

Similarly, we also have $B_2^\tau \sim (\sigma'_{B2}(\tau), \rho_{B1})$, where

$$\sigma'_{B2}(\tau) = \sigma_{B1} + \rho_{B1} \cdot \frac{\sigma_{D1} + \gamma_{11}\sigma_{A2}(\tau) + \delta_{11}}{R_2 - \rho_{D1} - \gamma_{11}\rho_{A1}}.$$

Using Lemma 7, we have $\sigma_{A2}(\tau) \leq \sigma'_{A2}(\tau)$ and $\sigma_{B2}(\tau) \leq \sigma'_{B2}(\tau)$. Solving these two inequalities, we can find that $\sigma_{A2}(\tau) \leq \sigma''_{A2}$, where

$$\sigma''_{A2} = \frac{\sigma_{A1} + \gamma_{A1}(\sigma_{C1} + \delta_{22}) + \gamma_{A1}\gamma_{22}(\sigma_{B1} + \gamma_{B1}(\sigma_{D1} + \delta_{11}))}{1 - \gamma_{11}\gamma_{B1}\gamma_{22}\gamma_{A1}},$$

and $\gamma_{A1} = \frac{\rho_{A1}}{R_1 - \rho_{C1} - \gamma_{22}\rho_{B1}}$, $\gamma_{B1} = \frac{\rho_{B1}}{R_2 - \rho_{D1} - \gamma_{11}\rho_{A1}}$. Note that σ''_{A2} is independent of τ. Similarly, we can derive an upper bound on $\sigma_{B2}(\tau)$, which is also independent of τ and can be denoted by σ''_{B2}.

After applying the technique of introducing stopped sequences and finding burstiness bounds for $A_2(t)$ and $B_2(t)$ that are independent of τ, we are now able to find out the burstiness bound on $A_4(t)$. The left-over service curve offered to A_3 by AP2 is denoted by $\beta_{A3}(t)$ and given by

$$\beta_{A3}(t) = (R_2 t - (\sigma_{D1} + \rho_{D1} t + \sigma_{B1} + \rho_{B1} t))^+.$$

Therefore, we have $A_4 \sim (\sigma_{A4}, \rho_{A1})$, where

$$\sigma_{A4} = \gamma_{11}\sigma''_{A2} + \delta_{11} + \gamma_{11}\rho_{11}\frac{\sigma_{D1} + \sigma_{B1}}{R_2 - \rho_{D1} - \rho_{B1}}.$$

It is trivial to find that $A_3(t) \sim (\gamma_{11}\sigma''_{A2} + \delta_{11}, \gamma_{11}\rho_{A1})$. In fact, worst-case buffer requirement (i.e., deterministic upper bound on backlog) at each individual AP can be found using our proposed framework. Furthermore,our approach allows for a fine-grained understanding of the worst-case buffer requirements for individual APs since the impacts of and interactions between different flows (i.e., $A_1(t), B_1(t), C_1(t)$, and $D_1(t)$) can now be quantitatively assessed.

Finally, the worst-case delay d_{A1} experienced by packets from A_1 that passes through both APs is upper bounded by the sum of the delay bounds induced by AP1 and AP2, i.e.,

$$d_{A1} = d_{left}^{A1} + d_{right}^{A1}.$$

At AP1, the left-over service for $A_1(t)$, which needs to be independent of τ, can now be derived. Let us denote this left-over service curve by $\beta_{A1}(t)$. By applying Theorem 2, we obtain

$$\beta_{A1}(t) = (R_1 t - (\rho_{C1} t + \sigma_{C1} + \gamma_{22}\sigma''_{B2} + \delta_{22} + \gamma_{22}\rho_{B1} t))^+.$$

Then, we can apply Theorem 4 and obtain

$$d_{left}^{A1} = \frac{\sigma_{A1} + \sigma_{C1} + \gamma_{22}\sigma''_{B2} + \delta_{22}}{R_1 - \rho_{C1} - \gamma_{22}\rho_{B1}}.$$

At AP2, we have already obtained the left-over service curve for $A_3(t)$ and its arrival curve. By applying Theorem 4 again, we have

$$d_{right}^{A1} = \frac{\gamma_{11}\sigma''_{A2} + \delta_{11} + \sigma_{D1} + \sigma_{B1}}{R_2 - \rho_{D1} - \rho_{B1}}.$$

Note that the delay bound d_{A1} is independent of τ, i.e., a closed-form expression of the worst-case delay bound for the wireless path is found. Since the closed-form expressions given by our proposed approach can be formally proved using network calculus theorems (see Sec. III), the derived bounds are reliable as long as the assumptions of our framework are carefully met and values for the parameters of our models are properly selected.

V. Numerical Evaluation

A. Experiment Settings

To demonstrate the use of our proposed framework, we consider a wireless PRP network designed for streaming phasor measurements. In [7], [22], it is reported that the size of phasor measurement packets is 300 bytes, with one packet every 20 ms. The wireless PRP network is depicted in Fig. 1 and its network calculus model is shwon Fig. 3. Our flow of interest is $A_1(t)$. Suppose that flow $B_1(t)$ is also a stream of phasor measurements with the same packet size and rate. If no other tasks generate any network traffic, i.e., $A_1(t)$, $B_1(t)$ only contain phasor measurements and $C_1(t)$, $D_1(t)$ contain no packets, we can model this application scenario using the following parameter values: $\sigma_{C1} = \sigma_{D1} = 0$, $\rho_{C1} = \rho_{D1} = 0$, γ_{11}=γ_{12}=γ_{21}=γ_{22}=1, δ_{11}=δ_{12}=δ_{21}=δ_{22}=0, σ_{A1}=σ_{B1}=2400 bps, and $\rho_{A1} = \rho_{B1} = 120000$ bps. We assume that IEEE 802.11b is used [7], and the raw data rates (i.e., values of R_1 and R_2) are 1 Mbps, 5.5 Mbps, or 11 Mbps.

B. Worst-Case Delays at Different Raw Data Rates

Under the scenario described in Sec. V-A, worst-case delay bounds at different raw data rates are listed in Table I. The delay bounds given by our proposed framework show that the wireless PRP network in Fig. 1 is suitable for streaming phasor measurement data, which typically requires worst-case end-to-end delays of 3 ms. The theoretical results agree with measurements obtained in [7]. With delay bounds derived by our framework, ICS architects/designers can choose proper raw data rates under various design constraints (e.g., end-to-end delay requirements, power consumption constraints).

TABLE I
Worst-Case Delay Bounds at Different Raw Data Rates

Raw Data Rate	1 Mbps	5.5 Mbps	11 Mbps
Delay Bound ($A_1 t$)	0.9776 ms	0.1751 ms	0.0874 ms

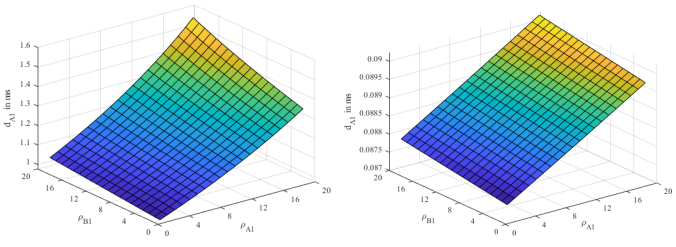

(a) R_1=R_2=1 Mbps. (b) R_1=R_2=11 Mbps.

Fig. 4. Impacts of the number of phasor measurement units on worst-case network-induced delays.

C. Impacts of the Number of Phasor Measurement Units

Suppose that we want to deploy more phasor measurement units into the system and that traffic profile of each unit remains the same. Fig. 4 shows the worst-case delay bounds when the number of phasor measurement units connected to each wireless access point varies from 1 to 20. As shown in Fig. 4(b), worst-case latency for phasor measurement packets is as low as 0.0902 ms when each wireless access point has 20 phasor measurement units and the raw data rate is 11 Mbps. On the other hand, Fig. 4(a) shows that the worst-case delay bound is 1.5547 ms when the raw data rate is reduced to 1 Mbps. At this low rate, our framework can help ICS architects find out that the number of phasor measurement units cannot exceed 37 at each access point if the worst-case delay requirement for the phasor data streaming application is 3 ms. When the raw data rate is low, it is therefore important to analyze worst-case delays of wireless PRP network infrastructure for applications with stringent worst-case delay requirements.

D. Impacts of Non-Latency-Critical Tasks

In addition to phasor data, network traffic generated by non-latency-critical tasks may also be carried by the wireless PRP network. Suppose that phasor measurement units at each wireless access point are occasionally reconfigured by the ICS system operators via the wireless PRP network. This task is not latency-critical and occurs infrequently, but its bursty traffic (i.e., large network packets containing configuration data) can impose additional queueing delays for phasor measurement data steams. If two operators reconfigure the phasor measurement units at both wireless access points simultaneously, we can model the generated traffic with $C_1(t)$ and $D_1(t)$. Since this task is infrequent, we approximate the average rates with $\rho_{C1} = \rho_{D1} = 0$. The burstiness components, σ_{C1} and σ_{D1}, model the bursty network packets containing configuration data. Suppose that size of these configuration data packets varies from 500 to 1500 bytes and that each wireless access point has only one phasor measurement unit connected to it. Fig. 5 shows the worst-case delay bounds derived by our framework with raw data rates of 1 Mbps and 11 Mbps.

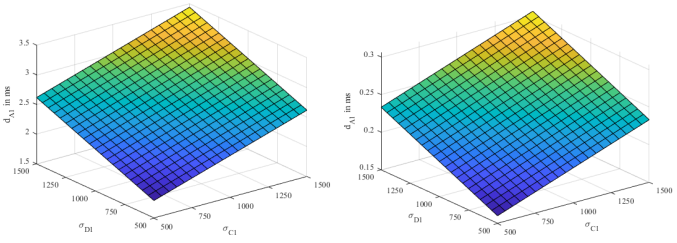

(a) R_1=R_2=1 Mbps. (b) R_1=R_2=11 Mbps.

Fig. 5. Impacts of bursty traffic from non-latency-critical tasks on worst-case network-induced delays.

At 11 Mbps, the newly introduced configuration task causes the worst-case delay bound for the flow of interest to increase from 0.0874 ms to 0.3061 ms, which is still far below the worst-case delay requirement of 3 ms. However, when the raw data rate is reduced to 1 Mbps, it is shown in Fig. 5(a) that a 1500-byte bursty configuration data packet causes a significant increase in worst-case delay for the flow of interest from 0.9776 ms to 3.4366 ms, which exceeds the worst-case delay requirement. Therefore, traffic regulation mechanism (e.g., constraining the maximum packet size to 1000 bytes) may need to be introduced when the wireless PRP network carries both phasor measurement data and configuration data at raw data rates of 1 Mbps.

VI. Conclusion and Future Work

In this work, we apply deterministic network calculus to model wireless PRP network infrastructure and show that closed-form expressions of network-induced worst-case end-to-end delays can be found for practical scenarios with non-feedforward traffic patterns, which has not been derived in prior research. Our current work only focuses on wireless path consisting of two APs, which are widely employed and studied in different ICS applications (e.g., [7], [14], [15]). As our future work, we will derive analytical delay bounds for sophisticated scenarios where the wireless path is comprised of more than two APs, which may be encountered in future ICSs spanning larger geographical regions. In addition, we will also try to further tighten the delay bounds provided by our framework, possibly through the use of piece-wise linear arrival and service curves introduced and studied in [17], [20].

Acknowledgment

This work is partially supported by NSF Award No. 1646458. Any opinions, findings, and conclusions or recommendations expressed in this paper are those of the author(s) and do not necessarily reflect the views of the sponsors of the research.

References

[1] F. Tramarin, S. Vitturi, M. Luvisotto, and A. Zanella, "On the Use of IEEE 802.11n for Industrial Communications," *IEEE Transactions on Industrial Informatics*, vol. 12, no. 5, pp. 1877–1886, October 2016.

[2] P. Park, S. C. Ergen, C. Fischione, C. Lu, and K. H. Johansson, "Wireless Network Design for Control Systems: A Survey," *IEEE Communications Surveys & Tutorials*, vol. 20, no. 2, pp. 978–1013, Second Quarter 2018.

[3] X. Li, D. Li, J. Wan, A. V. Vasilakos, C.-F. Lai, and S. Wang, "A Review of Industrial Wireless Networks in the Context of Industry 4.0," *Wireless Networks*, vol. 23, no. 1, pp. 23–41, January 2017.

[4] "Industrial Communication Networks - High Availability Automation Networks - Part 3: Parallel Redundancy Protocol (PRP) and High-Availability Seamless Redundancy (HSR)," International Electrotechnical Commission (IEC), IEC Standard, March 2016.

[5] M. Rentschler and P. Laukemann, "Performance Analysis of Parallel Redundant WLAN," in *2012 IEEE 17th International Conference on Emerging Technologies Factory Automation (ETFA 2012)*, September 2012, pp. 1–8.

[6] ——, "Towards a Reliable Parallel Redundant WLAN Black Channel," in *2012 9th IEEE International Workshop on Factory Communication Systems*, May 2012, pp. 255–264.

[7] M. Mohiuddin, M. Popovic, A. Giannakopoulos, and J. L. Boudec, "Experimental Validation of the Usability of Wi-Fi over Redundant Paths for Streaming Phasor Data," in *2016 IEEE International Conference on Smart Grid Communications (SmartGridComm)*, November 2016, pp. 533–538.

[8] M. Hendawy, M. ElMansoury, K. N. Tawfik, M. M. ElShenawy, A. H. Nagui, A. T. ElSayed, H. H. Halawa, R. M. Daoud, H. H. Amer, M. Rentschler, and H. M. ElSayed, "Application of Parallel Redundancy in a Wi-Fi-Based WNCS using OPNET," in *2014 IEEE 27th Canadian Conference on Electrical and Computer Engineering (CCECE)*, May 2014, pp. 1–6.

[9] "IEEE Standard Communication Delivery Time Performance Requirements for Electric Power Substation Automation," IEEE Standard, February 2005.

[10] M. Rentschler, H. H. Halawa, R. M. Daoud, H. H. Amer, A. T. ElSayed, A. H. Nagui, M. M. ElShenawy, K. N. Tawfik, M. ElMansoury, M. Hendawy, and H. M. ElSayed, "Simulative Comparison of Parallel Redundant Wireless Systems with OMNet++," in *2014 IEEE 23rd International Symposium on Industrial Electronics (ISIE)*, June 2014, pp. 1135–1140.

[11] G. Cena, S. Scanzio, and A. Valenzano, "Experimental Evaluation of Seamless Redundancy Applied to Industrial Wi-Fi Networks," *IEEE Transactions on Industrial Informatics*, vol. 13, no. 2, pp. 856–865, April 2017.

[12] A. Bouillard and G. Stea, "Exact Worst-Case Delay in FIFO-Multiplexing Feed-Forward Networks," *IEEE/ACM Transactions on Networking*, vol. 23, no. 5, pp. 1387–1400, October 2015.

[13] G. Cena, S. Scanzio, and A. Valenzano, "A Prototype Implementation of Wi-Fi Seamless Redundancy with Reactive Duplication Avoidance," in *2018 IEEE 23rd International Conference on Emerging Technologies and Factory Automation (ETFA)*, vol. 1, September 2018, pp. 179–186.

[14] M. M. Awad, H. H. Halawa, M. Rentschler, R. M. Daoud, and H. H. Amer, "Novel System Architecture for Railway Wireless Communications," in *IEEE EUROCON 2017 - 17th International Conference on Smart Technologies*, July 2017, pp. 877–882.

[15] B. Kilberg, C. B. Schindler, A. Sundararajan, A. Yang, and K. S. J. Pister, "Experimental Evaluation of Low-Latency Diversity Modes in IEEE 802.15.4 Networks," in *2018 IEEE 23rd International Conference on Emerging Technologies and Factory Automation (ETFA)*, vol. 1, September 2018, pp. 211–218.

[16] R. L. Cruz, "A Calculus for Network Delay, Part I: Network Elements in Isolation," *IEEE Transactions on Information Theory*, vol. 37, no. 1, pp. 114–131, January 1991.

[17] C.-S. Chang, *Performance Guarantees in Communication Networks*. Springer-Verlag, 2000.

[18] J.-Y. L. Boudec and P. Thiran, *Network Calculus: A Theory of Deterministic Queuing Systems for the Internet*. Springer-Verlag, 2001.

[19] J. B. Schmitt, F. A. Zdarsky, and L. Thiele, "A Comprehensive Worst-Case Calculus for Wireless Sensor Networks with In-Network Processing," in *Proceedings of the 28th IEEE International Real-Time Systems Symposium (RTSS 2007)*, Dec 2007, pp. 193–202.

[20] J. B. Schmitt, F. A. Zdarsky, and M. Fidler, "Delay Bounds under Arbitrary Multiplexing: When Network Calculus Leaves You in the Lurch..." in *Proc. IEEE INFOCOM 2008*, April 2008, pp. 1669–1677.

[21] S. Bondorf, P. Nikolaus, and J. B. Schmitt, "Quality and Cost of Deterministic Network Calculus: Design and Evaluation of an Accurate and Fast Analysis," *Proc. ACM Meas. Anal. Comput. Syst.*, vol. 1, no. 1, pp. 16:1–16:34, June 2017.

[22] M. Pignati, M. Popovic, S. Barreto, R. Cherkaoui, G. D. Flores, J. L. Boudec, M. Mohiuddin, M. Paolone, P. Romano, S. Sarri, T. Tesfay, D. Tomozei, and L. Zanni, "Real-Time State Estimation of the EPFL-Campus Medium-Voltage Grid by Using PMUs," in *2015 IEEE Power Energy Society Innovative Smart Grid Technologies Conference (ISGT)*, February 2015, pp. 1–5.